ACS OMEGA

Open Access

http://pubs.acs.org/journal/acsodf

Article

Formulation of Silymarin-β Cyclodextrin-TPGS Inclusion Complex: Physicochemical Characterization, Molecular Docking, and Cell Viability Assessment against Breast Cancer Cell Lines

Syed Sarim Imam,* Sultan Alshehri, Mohammad A. Altamimi, Wael A. Mahdi, and Wajhul Qamar

Cite This: https://doi.org/10.1021/acsomega.3c04225

Read Online

ACCESS | Metrics & More | Article Recommendations | Supporting Information

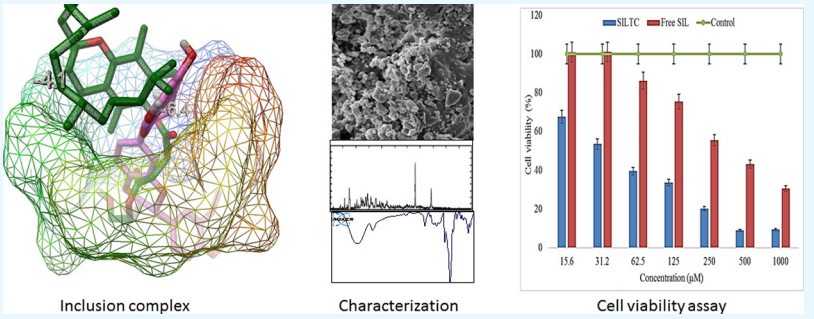

ABSTRACT: Silymarin (SIL) is a poorly water-soluble flavonoid reported for different pharmacological properties. Its therapeutic applications are limited due to poor water solubility. In this study, the solubility of silymarin has been enhanced by preparing freeze-dried binary and ternary complexes using beta cyclodextrin (βCD) and D-α-tocopherol polyethylene glycol 1000 succinate (TPGS). The stoichiometry of the drug and the carrier was selected from the phase solubility study. The dissolution study was performed to assess the effect of complexation on the release pattern of SIL. The formation of inclusion complexes was confirmed by different physicochemical studies. Finally, a cell viability assay (MCF 7; breast cancer cell line) was performed to compare the activity with free SIL. The phase solubilization results revealed the formation of a stable complex (binary) with a stability constant and complexation efficiency (CE) value of 288 mol L^{-1} and 0.045%. The ternary sample depicted a significantly enhanced stability constant and CE value (890 mol L^{-1} and 0.14%). The release study results showed a marked increase in the release pattern after addition of βCD (alone) in the binary mixture (49.4 $\pm$ 3.1%) as well as inclusion complex (66.2 $\pm$ 3.2%) compared to free SIL (32.7 $\pm$ 1.85%). Furthermore, with the addition of TPGS in SIL-βCD (ternary), the SIL release was found to be significantly enhanced from the SIL ternary mixture (79.2 $\pm$ 2.13%) in 120 min. However, fast SIL release was achieved with 99.2 $\pm$ 1.7% in 45 min for the SIL ternary complex. IR and NMR spectral analysis results revealed the formation of a stable complex with no drug−polymer interaction. The formation of complexes was also confirmed by the molecular docking study (docking scores of 4.1 and −6.4 kcal/mol). The in vitro cell viability result showed a concentration-dependent activity. The IC_{50} value of the SIL ternary complex was found to be significantly lower than that of free SIL. The findings of the study concluded that the prepared SIL inclusion complex can be used as an alternative oral delivery system to enhance solubility, dissolution, and biological activity against the tested cancer cell line.

INTRODUCTION

Silymarin (SIL) is a blend of four isomeric flavonoids (Figure 1A). It is derived from the milk thistle plant's seeds and fruit. It has been reported to have low oral bioavailability, and the systemic absorption is about 23−47%.[1,2] Factors like poor water solubility, poor intestinal absorption, and instability in the gastric environment may be the reason for poor bioavailability.[3,4] The drugs with low water solubility have been associated with low biological availability due to their dissolution as a rate-limiting step for the manifestation of bioactivity.[5] To overcome these problems, very high amounts of SIL are needed to achieve biological activity. There are a plethora of research articles that report the solubility enhancement of different drugs by using formulation approaches like cyclodextrin (CD) inclusion complex,[3,6] solid dispersions,[7−9] liposomes,[10,11] microbeads,[12] and nanoparticles.[13,14]

They have shown the linkage between the solubility and bioavailability enhancement because of poor SIL solubility

Received: June 14, 2023
Accepted: August 29, 2023

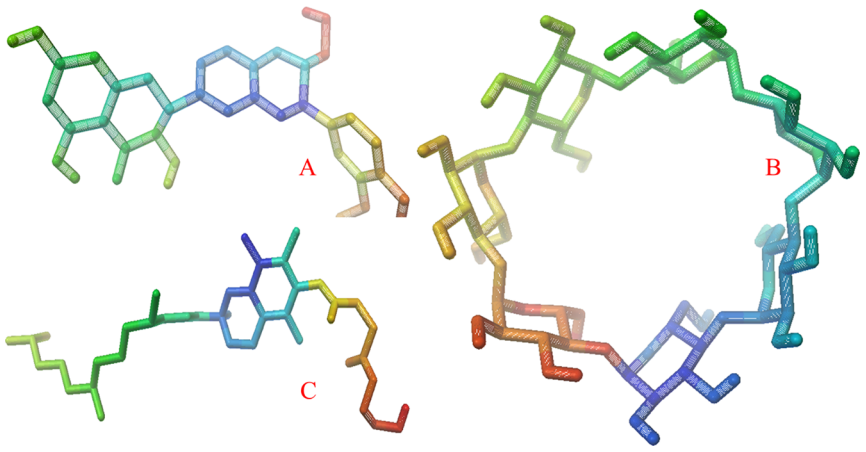

Figure 1. Chemical structure of SIL (A), βCD (B), and TPGS (C).

leading to limited drug absorption.[7,15] SIL solid dispersion was prepared by the freeze-drying method and reported significantly higher drug release than free SIL and physical mixture. It also reported many folds enhancement (215 and 589%) in the relative bioavailability as compared to the physical mixture and free SIL.[9] In another study, SIL solid dispersions were developed using the carrier polyvinylpyrrolidone-polyethylene glycol to increase the aqueous solubility. Both the carriers significantly affected the aqueous solubility and dissolution rate of SIL. They have reported ~1150-fold enhancement in solubility with this formulation compared to plain SIL powder.[8] Another research group reported the enhanced solubility of SIL by preparing solid dispersions using D-α-tocopherol polyethylene glycol 1000 succinate (TPGS) as a carrier. They have reported marked increase in the solubility from the SIL-solid dispersion group by 23-fold compared with the SIL group. They have also reported greater permeation by 4.6-fold, and its efflux ratio decreased from 5.5 to 0.6 in the presence of TPGS.[7] The solubility enhancement of SIL was also reported by the formulation of the inclusion complex.[6] They have reported that the formulation prepared with beta cyclodextrin (βCD) showed many folds increase in drug release than free SIL. In another research study, SIL inclusion complex was prepared with hydroxypropyl β CD and randomly methylated βCD.[3] They have reported that the complexation with these two CDs shows better results as an oral delivery system. It showed a potential therapeutic efficacy in the treatment of liver fibrosis. It has been used in conventional therapy and demonstrates antioxidant, anti-inflammatory, and anticancer effects. It also can cause some cells to undergo apoptosis. It acts as an antineoplastic agent in prostate, ovarian, lung, skin, bladder, and breast cancers and other malignancies.[16,17]

CD (Figure 1B) and its derivatives are well-known solubilizers with solubility-enhancing capabilities for drugs that are not soluble in water.[18] CDs are cyclic oligosaccharides with (1−4) glucosidic linkages connecting at least 6 D(+)glucopyranose units to each other. These cyclic glucopyranose molecules form a hollow cone with an external surface that is hydrophilic and an inner cavity that is lipophilic.[19,20] Its cavity size has a diameter of 6.0−6.5 and a volume of 265 Å^3,[21] and it is found suitable for different guest molecules having molecular weights between 200 and 800 g/mol.[22] In this inclusion mechanism, a lipophilic component forms a complex with the interior cavity of the CDs to enhance the solubility of the drug. Compounds can also be dissolved by CDs using simple techniques to form drug-CD complexes.[23,24] A high concentration of CD was necessary to formulate a formulation because of the high molecular weight of CD. Due to its potential toxicity and other associated side effects, the utilization of its high content may be restricted to use in delivery systems.[25] However, the low aqueous solubility of βCD is a problem for its use in drug-delivery systems.[26] The structural and functional modifications of βCD can further enhance the drug solubilization and inclusion properties due to availability of different reactive functional groups.[27,28] They enhance the aqueous solubility and wettability of poorly water-soluble drugs.[29]

According to recent reports, using a ternary system with a drug, CD, and a third auxiliary material can both lower the CD content and improve the complexation effectiveness.[25,26] There are numerous ternary substances used to prepare and evaluate inclusion complexes of poorly soluble drugs.[30−32] A novel highly water-soluble lipid-based nonionic surfactant approved as a safe excipient by the USFDA is TPGS (Figure 1C). It also has P-gp inhibitory effects and is well known to improve the solubility and bioavailability of drugs that are insoluble in water.[33,34] There is currently no literature describing the application of TPGS as a ternary substance in the formulation of inclusion complex of SIL with CD.

Using the freeze-drying technique, binary (SIL-CD) and ternary (SIL-CD-TPGS) SIL inclusion complexes were prepared in the current study design. The physical and chemical characteristics, dissolution, and cell line investigations of the prepared samples were assessed. The outcomes were compared with those of the physical mixture and free SIL. The molecular docking study evaluated the molecular formation mechanism.

MATERIALS

SIL and βCD were procured from Sigma Chemicals., M.O, USA. TPGS was purchased from Wuhan Jason Biotech Co., Ltd. (Wuhan, Hubei, China). Tween 80 and ethanol were procured from Applichem, Panreac, Darmstadt, Germany, and Eurostar Scientific Ltd. Liverpool L3 4BL, United Kingdom.

EXPERIMENTAL SECTION

Phase Solubility Study. This method was used to determine the stability constant and CE between the drug and the carrier. The binary (SIL-βCD) and ternary (SIL-βCD-TPGS) samples were used, and assessment was done as per the reported procedure with slight modifications.[35] 25 mL of double-distilled water was taken in a volumetric flask, and βCD

https://doi.org/10.1021/acsomega.3c04225
ACS Omega XXXX, XXX, XXX−XXX

(0−20 mM) was added for binary samples. Separately, a volumetric flask was also prepared for a ternary sample with the addition of TPGS (0.05%). An excess of SIL was added to each volumetric flask and kept on a water bath shaker for 72 h (25 °C). After the study was completed, the aliquots were collected and filtered. The total SIL concentration in each sample was analyzed after appropriate dilution using a UV spectrophotometer. The graph was plotted between the βCD concentration and the SIL concentration to calculate the stability constant (K_s) and the CE using the formula:[36]

$$K_c = \frac{\text{slope}}{\text{So}(1 - \text{slope})} \quad (1)$$

So, water solubility of SIL without the excipient

$$\text{CE} = \frac{\text{slope}}{1 - \text{slope}} \quad (2)$$

Formulation of Binary and Ternary Inclusion Complexes. The binary (SIL-βCD; 1:1 M; SILBC) and ternary (SIL-βCD-TPGS 1:1 M: 0.05%; SILTC) formulations were prepared by the freeze-drying method.[34] The composition of the inclusion complex is shown in Table 1. SIL was dissolved in the required volume of ethanol, and separately, βCD was dissolved in distilled water. In the case of ternary complex, TPGS was dissolved in βCD solution. Both solutions were mixed and stirred using a magnetic stirrer for 24 h to evaporate the organic solution. After that, the samples were frozen at −20 °C, followed by freeze drying. The freeze-dried SILBC and SILTC were collected and kept in the oven for 48 h at 40 °C to remove the moisture. Finally, the samples were transferred into glass vials and stored in a desiccator for further characterization.

Table 1. Formulation Composition of SIL Binary and Ternary Inclusion Complexes

formulation codes	SIL mol	βCD mol	TPGS %
SILBC	1	1	
SILTC	1	1	0.05
SILBM	1	1	
SILTM	1	1	0.05

Physical Mixture. The binary (SIL-βCD; 1:1 M; SILBM) and ternary (SIL-βCD-TPGS, 1:1 M: 0.05%; SILTM) physical mixtures were prepared by grinding in a mortar and pastel (Table 1). SIL and βCD were mixed and physically grinded for uniform mixing. In case of ternary mixture, TPGS was also added to the binary mixture and grinded for a few minutes for complete mixing. Finally, the binary and ternary mixtures were collected and stored for further characterization.

Drug Content. The prepared SILBM, SILBC, SILTM, and SILTC were evaluated for drug content to measure the presence of SIL in the prepared samples. The binary and ternary samples were taken in a volumetric flask, and methanol was added. The suspension was sonicated, and the volume was made up to 50 mL. The samples were filtered and diluted appropriately to measure the SIL concentration using a spectrophotometer.

Dissolution Study. The dissolution rate studies of free SIL and different prepared samples (SILBC, SILBM, SILTM, and SILTC) were performed using a dissolution apparatus (Distek Dissolution System 2500, North Brunswick, NJ) at a temperature of 37 ± 0.5 °C at 100 rpm. Each sample containing equivalent to 15 mg of SIL was taken in empty capsules and added to the phosphate buffer (pH 6.8) with 0.5% tween 80 (volume 900 mL). The released aliquots (5 mL) were collected and replaced with the same volume. The collected samples were filtered, diluted, and analyzed using a spectrophotometer.[14] The absorbance was used to calculate the concentration of SIL at each time point using the linear calibration plot (Supplementary Figure S1). Finally, the graph was plotted between time and concentration, and the measured data were used to calculate different release parameters.

Infrared Spectroscopy. The samples (pure SIL, βCD, TPGS, SILTM, and SILTC) were analyzed for FTIR in the range 400−4000 cm^{-1} using ATR (ATR-FTIR, Bruker Alpha, Germany). The test samples were scanned to analyze the characteristic peaks of free SIL and the changes observed after formulation into the inclusion complex. The characteristic peaks of SIL (Supplementary Figure S2) and shifts in their position on inclusion in the CD cavity are compared.

Nuclear Magnetic Resonance. The analysis was performed to evaluate the formation of an inclusion complex between SIL and the components. It was also used to assess the drug−carrier interaction. Each sample was individually scanned, and then the prepared physical mixture (SILTM) and inclusion complex (SILTC) were evaluated to assess the change in the characteristic spectra. The samples were scanned using an NMR instrument (Bruker; Switzerland). Deuterated DMSO was used as a solvent to prepare the samples.

Molecular Docking. Using Autodock 4.2 and Easydock Vina 2.2, molecular modeling of SIL-βCD-TPGS was performed. The geometry of the SIL and TPGS ligand structures was optimized using the Chem 3D 14.0 software. From the PDB cocrystal of amylase (PDB code: 1BFN, resolution 2.07), the crystal structure of the CD crystal was obtained and extracted. Autodock Tools (ADT) version 1.5.6 (www.autodock.scrips.edu) was used to dock the binary complex of SIL with the CD cavity. The following docking of the binary complex with TPGS (ternary complex) was performed.

Scanning Electron Microscopy. The analysis of free SIL and SILTC was performed with an electron microscope (JOEL, Tokyo, Japan). The samples were taken and spread over the holder with a double-adhesive tape, and the micrographs were collected to assess the change in morphology.

Differential Scanning Calorimetry. The free SIL, βCD, SILTM, and SILTC were analyzed by differential scanning calorimetry (DSC, Perkin Elmer Instruments, Bridgeport Avenue, Shelton, USA) to check the effect of excipient on the formulation. The thermal behavior was studied by heating about 5 mg of samples in a sealed aluminum pan. A stream of nitrogen was supplied, and scanning was performed in the temperature range of 30−300 °C with a heating rate of 10 °C/min.

X-ray Diffraction. The X-ray diffraction (XRD) patterns of free SIL, βCD, SILTM, and SILTC were evaluated using a diffractometer (Ultima IV diffractometer, Rigaku, Japan). The diffraction pattern of free SIL was compared with the prepared SILTM and SILTC. This helps to identify the changes in the crystallinity of the free drug compared to the inclusion complex.

Cell Viability Study. 3-(4,5-Dimethylthiazol-2-yl)-2,5-diphenyl tetrazolium bromide (MTT) assay method was used to evaluate the cell viability study using the breast cancer cell line (MCF 7). This technique relies on mitochondrial dehydrogenases to transform MTT into formazan crystals. The cells were grown in a 96-well plate using Dulbecco's modified Eagle's medium (10% fetal bovine serum) at a growth rate of 15,000 cells per well. The growth of the cells was done with a flow of

https://doi.org/10.1021/acsomega.3c04225
ACS Omega XXXX, XXX, XXX−XXX

CO_2 (5%) after the incubation of cells for 24 h. To test the viability of the cells, varied molar concentrations (from low to high) of free SIL and SILTC were added to the well. The samples were incubated in an incubator for 4 h so that live cells could metabolize the MTT. After replacing the media in each well, formazan was dissolved with DMSO. The plate was incubated, and an estimation using DMSO as a blank was done at 570 nm. The formula used to represent the fraction of viable cells is

$$\text{Cell viability (\%)} = \frac{\text{OD of treated cells}}{\text{OD of control cells}} \times 100 \quad (3)$$

Statistical Analysis. The experiment was performed in triplicate and shown as mean ± SD. One-way ANOVA was used to compare the two groups, and $p < 0.05$ was considered as significant.

RESULTS AND DISCUSSION

Phase Solubility Study. The graph was plotted between the concentration of βCD (with and without TPGS) and the concentration of SIL (Figure 2). Free SIL depicted an aqueous

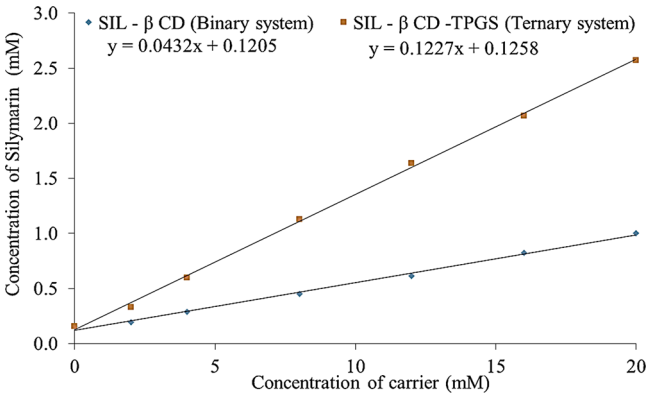

Figure 2. Phase solubility graph of binary (SIL-βCD) and ternary (SIL-βCD-TPGS) samples.

solubility of 75.77 ± 1.79 μg/mL, which is closer to the reported value.[37] The binary sample showed a stability constant and a CE value of 288 mol L^{-1} and 0.045, respectively. After adding different concentrations of CD, the aqueous solubility of SIL increased many folds, inferring that the formed complexes were reasonably stable.[38] The formed complex with a stability constant (K_s) value between 100 and 1000 M^{-1} would exhibit biological applications. The drug/CD system is unstable when the stability constant value is less than 100 M^{-1}. When the value is more than 1000 M^{-1}, it affects drug absorption. Furthermore, adding ternary substances (fixed concentrations of TPGS) leads to significant enhancements in the stability constant and CE. It showed a stability constant and CE value of 890 mol L^{-1} and 0.14, respectively. TPGS interacts with the outer surface of the CD torus as well as with the drug-CD systems that display higher K_s and CE.[18] The phase solubility diagram was found to be of three types based on solubility: A_L type (increase in CD concentration led to drug enhancement), A_P type (CD more effective at high concentrations), and A_N type (negatively deviated straight line due to CD is more effective at low concentrations). In this study, the graph was found to be of A_L type.[39] For both the binary and ternary systems, the slopes of the phase solubility curves were smaller than unity. It was hypothesized that the drug and CD would form 1:1 M stoichiometric inclusion complexes in solution.[40]

Drug Content. The drug content assay results showed that the prepared binary and ternary samples (SILBM, SILBC, SILTM, and SILTC) were found to be in the range of 85−95%. SILBM and SILBC showed drug contents of 85.8 ± 2.7 and 88.6 ± 2.1%, respectively. In the case of SIL ternary physical mixture (SILTM) and inclusion complex (SILTC), the drug contents were 91.45 ± 3.4 and 93.9 ± 2.9%, respectively. The physical mixture showed lesser SIL content in compared to the inclusion complex. The slight loss of SIL may be due to the formulation process. The difference was found to be nonsignificant.

Dissolution Study. The study of different samples was evaluated, and the data are shown in Figure 3. A significant

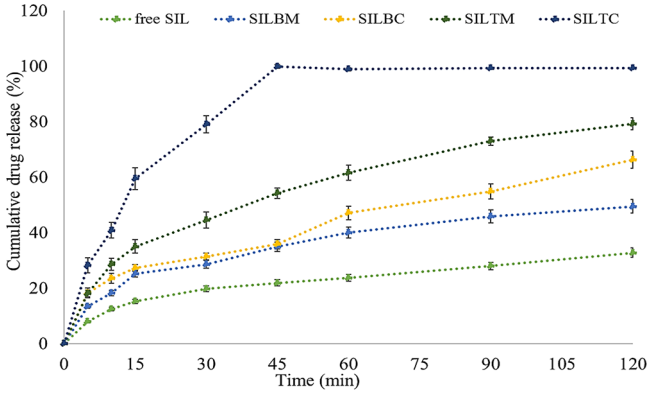

Figure 3. Dissolution profile of free SIL, binary (SILBM) and ternary mixture (SILTM), and SIL binary (SILBC) and ternary inclusion complex (SILTC). Study performed in triplicate and data shown as mean ± SD.

change in the release pattern was observed in the different samples at all time points compared to free SIL. The free SIL depicted a poor drug release pattern, with a maximum release of 32.7 ± 1.85% in 120 min. The poor release of SIL was found to be due to its hydrophobic property.[41] βCD has a surfactant-like property with hydrophilic properties on the outside surface. Thus, it promotes the dissolution rate by lowering the interfacial tension between the poorly soluble drug and the release medium.[42] The binary mixture significantly increases the release of SIL, with a maximum release of 49.1 ± 3.1%. The improvement in release was attained due to the reduction in the particle size of SIL after trituration with βCD. The increase in wettability and solubility of SIL at the initial stage of the release study was due to the coexistence of SIL and βCD in the dissolution medium.[26] In the case of the binary complex, the drug-release profile is significantly enhanced compared to free SIL, and the maximum drug release reaches 66.3 ± 3.2%. About 2-fold enhancement in release was achieved from SILBC than free SIL. The better SIL release was achieved from the binary complex due to the partial entrapment of drug molecules inside the βCD torus. The presence of CD leads to enhancement of the solubility of poorly soluble drugs after inclusion into the hydrophobic cavity. A better release profile for the binary complex was observed, which might be because of formation of a soluble complex with βCD and the improved hydrophilicity of SIL in the buffer. The enhancement in release was achieved due to the conversion to the high energetic amorphous state after complexation,[43] which imparts hydrophilic character.[26] The addition of the ternary compound TPGS in the ternary system

https://doi.org/10.1021/acsomega.3c04225
ACS Omega XXXX, XXX, XXX−XXX

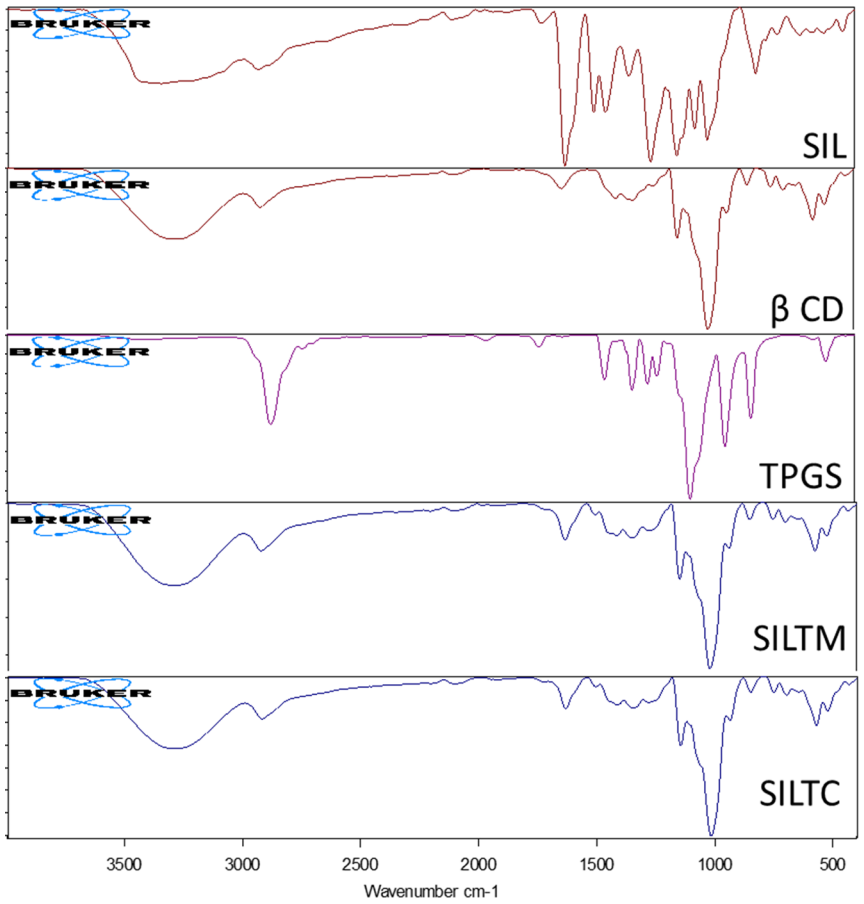

Figure 4. FTIR spectra of free SIL, βCD, TPGS, SILTM, and SILTC.

further enhances the release pattern from the binary mixture and inclusion complex. The ternary mixture showed greater SIL release compared to free SIL, the binary mixture, and the binary complex. The maximum SIL release was reached at 79.2 ± 2.3% within 120 min. The addition of TPGS with βCD showed a synergistic effect in solubility enhancement and promoted the release. It reduces the drug crystallinity to a greater extent than the binary mixture and inclusion complex. In the case of ternary complex, a fast and high dissolution rate was found. The maximum drug release of 99.2 ± 3.1% was achieved in the 45 min. of study, whereas the samples released only 35−55% of SIL in the same time. It releases about 40% SIL in the initial 10 min. The other samples released between 18 and 28% in the 10 min. The quick release was attributed to the better inclusion and CE of βCD achieved after the addition of TPGS to the binary mixture.

The in vitro release data were further evaluated for dissolution efficiency (DE) and mean dissolution time (MDT). The MDT and DE values for prepared samples were found to be significantly improved compared to free SIL. It is evident that all examined systems exhibited faster dissolution rates than the free drug. Free SIL demonstrated DE and MDT of 0.22% and 36.46 min. In the case of SILBM and SILBC, significantly better ($p < 0.01$) dissolution properties were observed than free SIL. They showed MDT values of 31.47 and 41.79 min, respectively. They showed DE values of 0.36 (1.6-fold higher) and 0.43 (1.95-fold higher) indicating a higher complexation and solubility of SIL. SILBC showed higher MDT and DE than the physical mixture in improving the drug dissolution behavior. The ternary mixture (SILTM) and ternary complex (SILTC) depicted 2.5- and 3.8-fold enhanced DE compared to free SIL, respectively. It also depicted about a 2-fold higher DE than the binary mixture and binary complex. The MDT was found to be 33.8 and 16.1 min for ternary mixtures and ternary complexes, respectively. Thus, the use of ternary substances confirms the synergistic increase of the drug solubility obtained when used in combination with βCD.[44]

Infrared Spectroscopy. The chemical structure of SIL with numbering and their depicted IR frequencies for the free SIL, TPGS, and βCD along with SILTM and SILTC are shown in Supplementary Table S1 and Figure 4. SIL is a flavolignan and a small subclass of compounds. The flavonoid moiety is fused with a lignan to form a flavolignan. The observed peaks for the free SIL were the stretching vibration at 3344.59 cm^{-1} for phenolic hydroxyl moieties at C-5, C-7, and C-20. The C-3 and C-2 hydroxyl groups exhibited their stretching vibration at 1079.70 cm^{-1}. It also exhibited stretching vibration peaks at 2932.98 cm^{-1} for the aromatic C−H group. The other manifested peaks for C═O and C−O−C stretching vibrations were observed at 1630.47 and 1458.82 cm^{-1}, respectively. The carrier βCD exhibited its stretching vibrations at 3280.41 cm^{-1} for the cyclic hydroxyl group and 1149.46 cm^{-1} for the C−O−C moiety. The observed stretching vibration frequency for the TPGS was exhibited at 2876.52 cm^{-1} for the ester moiety. It also exhibited an aromatic C═C stretching vibration at 1344.43 cm^{-1} and an obvious peak for C−O−C stretching vibration at 1098.11 cm^{-1}. The spectra of SILTM and SILTC showed the peaks for the hydroxyl moiety of the free SIL. The frequency for the ester group of the TPGS carrier was not observed in both prepared samples. The other peaks of the free SIL, along with the peaks of

https://doi.org/10.1021/acsomega.3c04225
ACS Omega XXXX, XXX, XXX−XXX

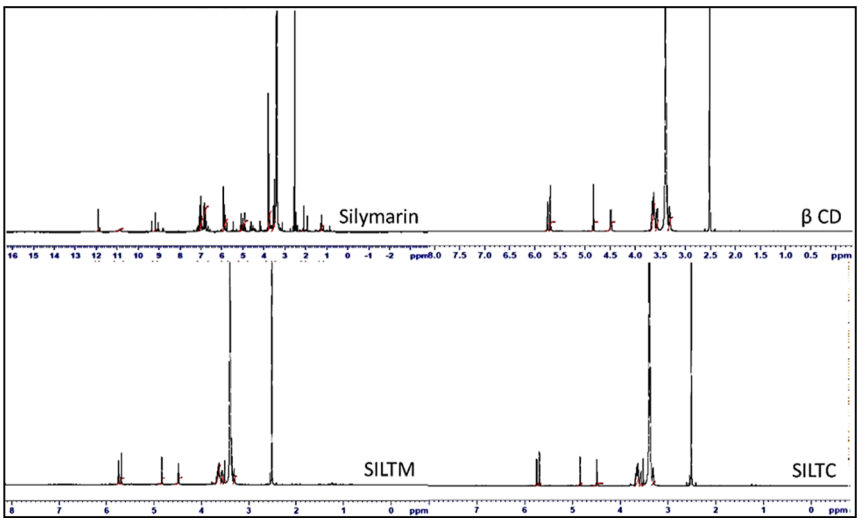

Figure 5. ^{1}H NMR spectra of free SIL, βCD, ternary physical mixture (SILTM), and ternary inclusion complex (SILTC).

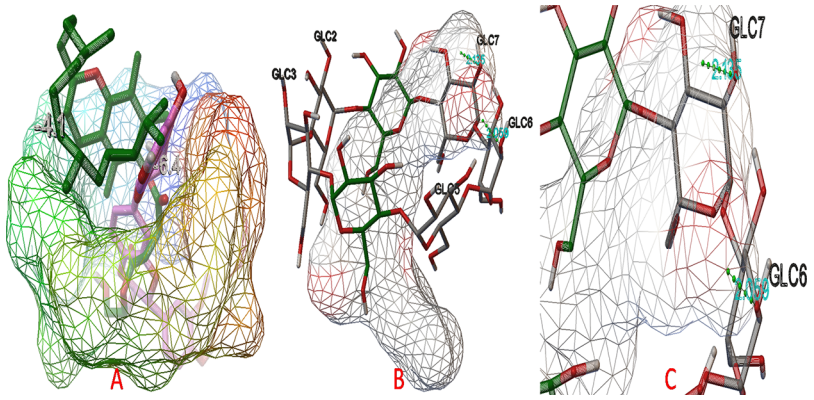

Figure 6. (A−C) Docking image of SIL with β CD and TPGS. (A) Binding affinity score of β CD with SIL (−6.4) and TPGS (−4.1). (B) Hydrogen bond interaction. (C) Zoom image of H-bond interaction of SIL with β CD.

the carriers, were visible in SILTM and SILTC, with a slight change in their frequency as depicted in the spectra. From the study, we can say that there was no interaction observed between the drug and the carrier in the physical mixture or inclusion complex. This change in spectra was also in compliance with the spectra of NMR.

NMR Study. ^{1}H NMR study of free SIL, βCD, and prepared formulations (SILTM and SILTC) was performed to investigate the relationship between the free drug and carriers, as depicted in Supplementary Table S2 and Figure 5. The chemical shift values of free SIL exhibited a definite deshielded singlet at δ 11.91 ppm, which is attributed to C-5, C-7, and C-20 of the hydroxyl moiety. The hydroxyl moiety at C-3 and C-23 exhibited a distinct peak at δ 9.18 ppm of the flavolignans. The aromatic carbon is depicted in the multiplet peaks at δ 5.0−7.1 ppm for the fused free pure drug. The methoxy group of the lignan moiety in the fused free drug is depicted in its recognizable peak at δ 4.18 ppm. The C−H moiety of 1.4-dioxane (C-10 and C-11) in lignan exhibited multiple peaks at δ 3.40−3.79 ppm. The carrier βCD exhibited its singlet peak at δ 5.75 ppm corresponding to position 1 of the glucose moiety. The other peaks of the glucose moiety were also visible in the given spectra. The chemical shift of the hydroxyl moiety for the βCD carrier depicted a singlet peak at δ 2.51 ppm. Taking into consideration the chemical shift (δ) values of both the prepared samples, they were in concordance with IR spectroscopy, as aforementioned. No chemical shift values for the hydroxyl peaks of the free SIL were observed, as found in the results of the IR spectra. The spectra also exhibited merged peaks at δ 5.69−5.75 ppm of free SIL and βCD in both SILTM and SILTC. The disappearance of some peaks may be due to the formation of the inclusion complex. The peaks of free SIL for 1.4-dioxane were also found to be merged at δ 3.3−3.67 ppm with the carrier. The singlet peak for the methoxy group was also observed, with a slight change at δ 4.83 ppm. The chemical shift of the hydroxyl group of the βCD was perceptible at δ 2.51 ppm with an insignificant change. As stated above, we conclude with the statement that, as per the above given spectral values, the change in the spectral value takes place due to the formation of ternary complexes. The findings of IR and NMR are also supported by molecular docking for the formation of inclusion complexes.

Molecular Docking Study. To have better results for the binding mode of the inclusion complexes, we have performed molecular docking to analyze the molecular interaction between the ligand and the carrier. In order to identify the best binding mode and conformations, Autodock 4.2 with Lamarckian genetic algorithm was used. The conformation of the two ligands (SIL and TPGS) attached to the βCD are shown in Figure 6A−C. The binding affinity of SIL at βCD was found to be −6.4 kcal/mol when docked. The two-hydrogen bonds were

https://doi.org/10.1021/acsomega.3c04225
ACS Omega XXXX, XXX, XXX−XXX

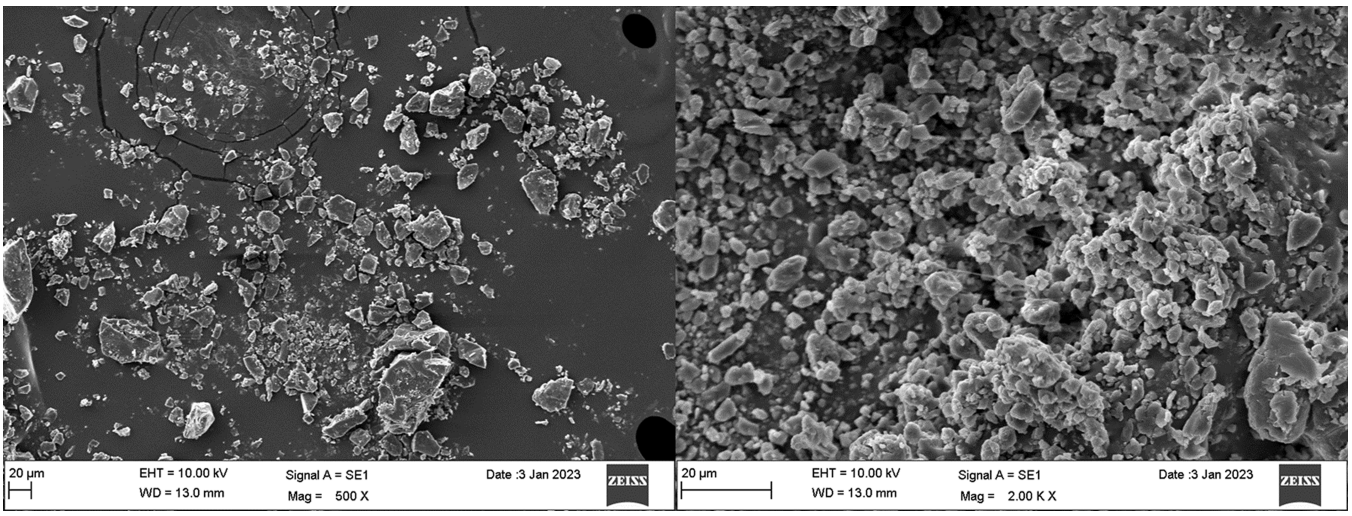

Figure 7. SEM image of free SIL and SILTC.

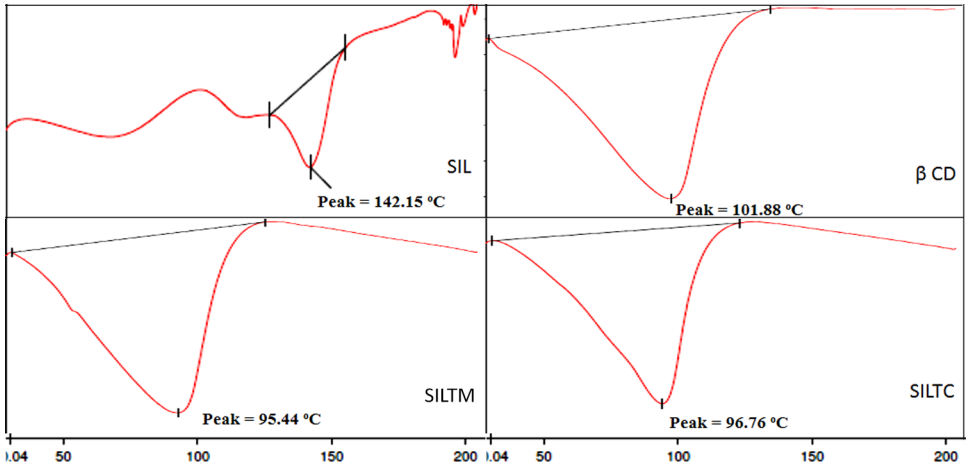

Figure 8. DSC thermogram of free SIL, βCD, SILTM, and SILTC.

formed when SIL was aligned in the CD central cavity, disclosing the binary interaction of the complex. The chromene ring extends out of the cavity, whereas the benzodioxin moiety settled at the βCD cavity. The 5,7-dihydroxyl substituent of the chromene moiety was found to construct a hydrogen bond with the glucose moiety of βCD, viz., GLC 6 and GLC 7, as illustrated in Figure 6B,C. The bond lengths of the two-hydrogen bonds were found to be at 2.135 and 2.059 Å. The hydrophobic portion of the βCD was occupied by the aromatic benzodioxin moiety of SIL. The supercilious ternary inclusion complex of SIL, βCD, and TPGS took a pose by docking TPGS into the SILBC. The TPGS binding affinity with the SIL-βCD complex was found to be −4.1 kcal/mol. The studies showing the molecular interaction of TPGS exhibited that the central cavity of the βCD was occupied by the chromenyl ring along with the aliphatic side chain. The protruding part outside the βCD was found to be the succinate and polyethylene glycol chains. The hydrophobic pocket of the CD exhibiting hydrophobic interaction was embedded by the aliphatic side chain of TPGS. The steric hindrance was found to be absent between SIL and TPGS moiety when compacted inside the CD cavity. This concludes that the ternary inclusion complex was assumed to be a thermodynamically stable complex.

Scanning Electron Microscopy. The photomicrographs of scanning electron microscopy (SEM) display the morphological patterns of both free SIL and a ternary complex (SILTC). The acicular, thin, and elongated SIL crystals are depicted in Figure 7. When an inclusion complex forms, just one component can be viewed.[45] However, in the micrographs of the ternary system, the typical patterns of free SIL crystals and CD have changed. This is due to a distinct, smaller-sized amorphous structure than that found in the components alone. These morphological and crystallographic alterations offer compelling proof that inclusion complexes have formed.

DSC. To further support the formation of the SIL complex, DSC was used to characterize it in the solid state and in the thermogram depicted in Figure 8. In free SIL, there was a sharp endothermic peak at 142 °C corresponding to the melting temperature of the drug.[46] The value was found to be closer to the reported melting point. βCD showed a broad endothermic peak at 101.1 °C, analogous to its reported melting temperature. In the case of ternary mixture (SILTM) and inclusion complex (SILTC), the endothermic peak of SIL vanished. There was a slight change in the peaks observed at 95.5 and 97.6 °C, found to be of βCD. The missing drug melting peak of SIL in SILTC gives strong evidence for the complete inclusion of drug into the carrier.

https://doi.org/10.1021/acsomega.3c04225
ACS Omega XXXX, XXX, XXX−XXX

XRD. The different samples were characterized using XRD, and the diffractograms of prepared samples (SILTM and SILTC) were compared with free SIL (Figure 9). Free SIL

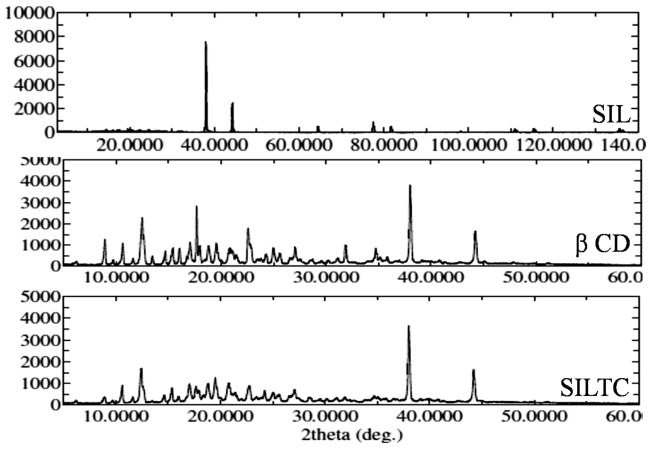

Figure 9. XRD diffractogram of free SIL, βCD, and SILTC.

showed high-intensity characteristic peaks, which confirm its crystallinity. The prepared sample of SILTM depicted the conversion of crystalline SIL into an amorphous form. There was a slight reduction in the peak intensity and shape (image not shown). However, in the case of SILTC, a significant change in the peak intensity and shape was observed. The free SIL peaks are completely superimposed by the peaks of the carrier βCD. The diffraction pattern was expected from the XRD data because the solubility was markedly enhanced after the formulation of the inclusion complex.

Cell Viability Assay. The cell viability study results reveal the concentration-dependent cytotoxicity of free SIL and SILTC against the breast cancer cell line (MCF 7). The study included lower concentration (15.6 μM) and higher concentration (1000 μM) of free SIL and SILTC. At the lowest concentration (15.6 μM), free SIL demonstrated no effect on cell viability, whereas with the prepared SILTC, a greater effect was observed (67.59%) at the same concentration (Figure 10). Free SIL showed the maximum cytotoxic effect at 1000 μM (30.43% viability), but a similar effect on cell viability was observed from SILTC at 125 μM; at 500 μM (8.93%) and 1000 μM (9.39%),

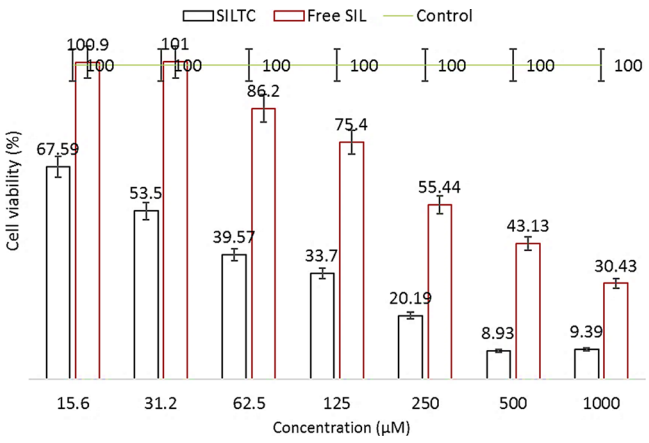

Figure 10. Cell viability assessment of free SIL and SIL inclusion complex against the breast cancer (MCF 7) cell line. Study performed in triplicate and data shown as mean ± SD.

the cell viability reached less than 10%. The maximum effect of SILTC was observed at 500 μM concentration. It can be observed that there is no significant difference in the effects of SILTC at 500 and 1000 μM. Free SIL also exhibited cytotoxic effects at different concentrations. However, they are weaker as compared with SILTC: 15.6 μM (100.9%), 31.2 μM (101%), 62.5 μM (86.2%), 125 μM (75.4%), 250 μM (55.44%), 500 μM (43.13%), and 1000 μM (30.43%). These in vitro cytotoxic effects on cancer cells may be attributed to the induction of apoptosis by SIL, as reported in the study by Kim et al.[47] They reported that SIL regulates the expression of apoptotic proteins in the breast cancer cell line causing apoptotic death and inhibiting proliferation. MAPK signaling pathways have also been reported to be involved in SIL-induced apoptosis in MCF-7 breast cancer cells. Based on these results, SIL was used to evaluate its effects on in vitro cell growth and proliferation in MCF-7 cells. Based on the absorbance readings after the MTT assay, the IC_{50} was calculated for SIL and SILTC. The values were found to be significantly different from each other. Free SIL showed an IC_{50} value of 562.7 μM, whereas the prepared SILTC demonstrated a significantly ($p < 0.001$) low IC_{50} value (59.85 μM). A 9.4-fold reduction was observed in the IC_{50} value when compared with SILTC. The reduction in the IC_{50} value and the enhancement in cytotoxicity may be due to the enhanced solubility of SIL in the used carrier.

CONCLUSIONS

In the current investigation, CD and TPGS (a ternary material) were used to produce a ternary inclusion complex that improved the solubility of SIL. The process of freeze drying was used to produce the inclusion complexes. The formation of a stable complex is confirmed by the high stability constant and the CE value. No drug−polymer interaction was seen in the IR and NMR spectral data. It received additional support from the molecular docking study result. The transformation of crystalline SIL into an amorphous state is confirmed by SEM, XRD, and DSC images. The results of the dissolution investigation showed a considerable improvement in the release pattern following complexation. According to the in vitro cell viability results, there was a concentration-dependent activity and a significant decrease in the IC_{50} value of the SIL inclusion complex observed. According to the study, the developed SIL inclusion complex is a new oral delivery strategy that can improve solubility, dissolution, and in vitro efficacy against breast cancer cell lines.

ASSOCIATED CONTENT

Supporting Information

The Supporting Information is available free of charge at https://pubs.acs.org/doi/10.1021/acsomega.3c04225.

Calibration plot of SIL over the concentration range used to calculate different parameters; chemical structure of the drug with their numbering and functional groups used to interpret the IR and NMR spectra; and IR and NMR spectra table of pure compounds as well as their formulations (PDF)

AUTHOR INFORMATION

Corresponding Author

Syed Sarim Imam − *Department of Pharmaceutics, College of Pharmacy, King Saud University, Riyadh 11451, Saudi*

https://doi.org/10.1021/acsomega.3c04225
ACS Omega XXXX, XXX, XXX−XXX

Arabia; orcid.org/0000-0002-8913-0826;
Email: simam@ksu.edu.sa

Authors

Sultan Alshehri − *Department of Pharmaceutics, College of Pharmacy, King Saud University, Riyadh 11451, Saudi Arabia;* orcid.org/0000-0002-0922-9819

Mohammad A. Altamimi − *Department of Pharmaceutics, College of Pharmacy, King Saud University, Riyadh 11451, Saudi Arabia*

Wael A. Mahdi − *Department of Pharmaceutics, College of Pharmacy, King Saud University, Riyadh 11451, Saudi Arabia;* orcid.org/0000-0002-7083-1753

Wajhul Qamar − *Department of Pharmacology and Toxicology, College of Pharmacy, King Saud University, Riyadh 11451, Saudi Arabia*

Complete contact information is available at:
https://pubs.acs.org/10.1021/acsomega.3c04225

Notes

The authors declare no competing financial interest.

■ ACKNOWLEDGMENTS

The authors extend their appreciation to the Researcher Promotion Scheme King Saud University, Saudi Arabia for funding this research work through the project no. RSP2023R146.

■ REFERENCES

(1) Wu, J. W.; Lin, L. C.; Hing, S. C.; Chi, C. W.; Tsai, T. H. Analysis of silibinin in rat plasma and bile for hepatobiliary excretion and oral bioavailability application. *J. Pharm. Biomed. Anal.* **2007**, *45*, 635−641.
(2) Ghosh, A.; Ghosh, T.; Jain, S. Silymarin-a review on the pharmacodynamics and bioavailability enhancement approaches. *J. Pharm. Sci. Technol.* **2010**, *2*, 348−355.
(3) Gharbia, S.; Balta, C.; Herman, H.; Rosu, M.; Váradi, J.; Bácskay, I.; Vecsernyés, M.; Gyongyosi, S.; Fenyvesi, F.; Voicu, S. N.; Stan, M. S.; Cristian, R. E.; Dinischiotu, A.; Hermenean, A. Enhancement of Silymarin Anti-fibrotic Effects by Complexation With Hydroxypropyl (HPβCD) and Randomly Methylated (RAMEB)-Cyclodextrins in a Mouse Model of Liver Fibrosis. *Front. Pharmacol.* **2018**, *9*, 883.
(4) Loguercio, C.; Festi, D. Silybin and the liver: from basic research to clinical practice. *World J. Gastroenterol.* **2011**, *17*, 2288−2301.
(5) Lee, J. S.; Hong, D. Y.; Kim, E. S.; Lee, H. G. Improving the water solubility and antimicrobial activity of silymarin by nanoencapsulation. *Colloids Surf., B* **2017**, *154*, 171−177.
(6) Ghosh, A.; Biswas, S.; Ghosh, T. Preparation and Evaluation of Silymarin β-cyclodextrin Molecular Inclusion Complexes. *J. Young Pharm.* **2011**, *3*, 205−210.
(7) Song, I. S.; Nam, S. J.; Jeon, J. H.; Park, S. J.; Choi, M. K. Enhanced Bioavailability and Efficacy of Silymarin Solid Dispersion in Rats with Acetaminophen-Induced Hepatotoxicity. *Pharmaceutics* **2021**, *13*, 628.
(8) Yousaf, A. M.; Malik, U. R.; Shahzad, Y.; Mahmood, T.; Hussain, T. Silymarin-laden PVP-PEG polymeric composite for enhanced aqueous solubility and dissolution rate: Preparation and in vitro characterization. *J. Pharm. Anal.* **2019**, *9*, 34−39.
(9) Lim, D. Y.; Pang, M.; Lee, J.; Lee, J.; Jeon, J. H.; Park, J. H.; Choi, M. K.; Song, I. S. Enhanced bioavailability and hepatoprotective effect of silymarin by preparing silymarin-loaded solid dispersion formulation using freeze-drying method. *Arch. Pharmacal Res.* **2022**, *45*, 743−760.
(10) Elmowafy, M.; Viitala, T.; Ibrahim, H. M.; Abu-Elyazid, S. K.; Samy, A.; Kassem, A. M.; Yliperttula, M. Silymarin loaded liposomes for hepatic targeting: in vitro evaluation and HepG2 drug uptake. *Eur. J. Pharm. Sci.* **2013**, *50*, 161−171.
(11) Kumar, N.; Rai, A.; Reddy, N. D.; Raj, P. V.; Jain, P.; Deshpande, P.; Mathew, G.; Kutty, N. G.; Udupa, N.; Rao, C. M. Silymarin liposomes improves oral bioavailability of silybin 4 besides targeting hepatocytes, and immune cells. *Pharmacol. Rep.* **2014**, *66*, 788−798.
(12) Ghosal, K.; Adak, S.; Agatemor, C.; Praveen, G.; Kalarikkal, N.; Thomas, S. Novel interpenetrating polymeric network-based microbeads for delivery of poorly water soluble drug. *J. Polym. Res.* **2020**, *27*, 98.
(13) Cengiz, M.; Kutlu, H. M.; Burukoglu, D. D.; Ayhanci, A. A comparative study on the therapeutic effects of silymarin and silymarin-loaded solid lipid nanoparticles on d-GaIN/TNF-a-induced liver damage in balb/c mice. *Food Chem. Toxicol.* **2015**, *77*, 93−100.
(14) El-Nahas, A. E.; Allam, A. N.; Abdelmonsif, D. A.; El-Kamel, A. H. Silymarin-Loaded Eudragit Nanoparticles: Formulation, Characterization, and Hepatoprotective and Toxicity Evaluation. *AAPS PharmSciTech* **2017**, *18*, 3076−3086.
(15) Di Costanzo, A.; Angelico, R. Formulation Strategies for Enhancing the Bioavailability of Silymarin: The State of the Art. *Molecules* **2019**, *24*, 2155.
(16) Hajighasemlou, S.; Farajollahi, M.; Alebouyeh, M.; Rastegar, H.; Manzari, M. T.; Milad-Mirmoghtadaei, M.; Moayedi, B.; Ahmadzadeh, M.; Kazemi, M.; Parvizpour, F.; Gharibzadeh, S. Study of the Effect of Silymarin on Viability of Breast Cancer Cell Lines. *Adv. Breast Cancer Res.* **2014**, *3*, 100−105.
(17) Sharma, G.; Singh, R. P.; Chan, D. C.; Agarwal, R. Silibinin Induces Growth Inhibition and Apoptotic Cell Death in Human Lung Carcinoma Cells. *Anticancer Res.* **2003**, *23*, 2649−2655.
(18) Marques, C. S. F.; Barreto, N. S.; Oliveira, S. S. C. d.; Santos, A. L. S.; Branquinha, M. H.; Sousa, D. P. d.; Castro, M.; Andrade, L. N.; Pereira, M. M.; Silva, C. F. d.; et al. β-Cyclodextrin/Isopentyl Caffeate Inclusion Complex: Synthesis, Characterization and Antileishmanial Activity. *Molecules* **2020**, *25*, 4181.
(19) Li, H.; Zhang, G.; Wang, W.; Chen, C.; Jiao, L.; Wu, W. Preparation, Characterization, and Bioavailability of Host-Guest Inclusion Complex of Ginsenoside Re with Gamma-Cyclodextrin. *Molecules* **2021**, *26*, 7227.
(20) Taupitz, T.; Dressman, J. B.; Buchanan, C. M.; Sandra, K. S. Cyclodextrin-water soluble polymer ternary complexes enhance the solubility and dissolution behaviour of poorly soluble drugs. Case example: Itraconazole. *Eur. J. Pharm. Biopharm.* **2013**, *83*, 378−387.
(21) Del Valle, E. M. Cyclodextrins and their uses: A review. *Process Biochem.* **2004**, *39*, 1033−1046.
(22) Liu, B.; Li, W.; Zhao, J.; Liu, Y.; Zhu, X.; Liang, G. Physicochemical characterisation of the supramolecular structure of luteolin/cyclodextrin inclusion complex. *Food Chem.* **2013**, *141*, 900−906.
(23) Loftsson, T.; Masson, M. The effects of water-soluble polymers on cyclodextrins and cyclodextrin solubilization of drugs. *J. Drug Delivery Sci. Technol.* **2004**, *14*, 35−43.
(24) Loftsson, T.; Messner, M.; Kurkov, S. V.; Brewster, M. E.; Jansook, P. Self-assembly of cyclodextrin complexes: aggregation of hydrocortisone/cyclodextrin complexes. *Int. J. Pharm.* **2011**, *407*, 174−183.
(25) Jug, M.; Becirevic-Lacan, M. Multicomponent complexes of piroxicam with cyclodextrins and hydroxypropyl methylcellulose. *Drug Dev. Ind. Pharm.* **2004**, *30*, 1051−1060.
(26) Bera, H.; Chekuri, S.; Sarkar, S.; Kumar, S.; Muvva, N. B.; Mothe, S.; Nadimpalli, J. Novel pimozide-β-cyclodextrin-polyvinylpyrrolidone inclusion complexes for Tourette syndrome treatment. *J. Mol. Liq.* **2016**, *215*, 135−143.
(27) Das, S. K.; Kahali, N.; Bose, A.; Khanam, J. Physicochemical characterization and in vitro dissolution performance of ibuprofen-Captisol (sulfobutylether sodium salt of β-CD) inclusion complexes. *J. Mol. Liq.* **2018**, *261*, 239−249.
(28) Pal, A.; Roy, S.; Kumar, A.; Mahmood, S.; Khodapanah, N.; Thomas, S.; Agatemor, C.; Ghosal, K. Physicochemical Characterization, Molecular Docking, and In Vitro Dissolution of Glimepiride−Captisol Inclusion Complexes. *ACS Omega* **2020**, *5*, 19968−19977.
(29) Uekama, K.; Hirayama, F.; Arima, H. Recent aspect of cyclodextrin-based drug delivery system. *J. Inclusion Phenom. Macrocyclic Chem.* **2006**, *56*, 3−8.

https://doi.org/10.1021/acsomega.3c04225
ACS Omega XXXX, XXX, XXX−XXX

(30) Donthi, M. R.; Munnangi, S. R.; Krishna, K. V.; Marathe, S. A.; Saha, R. N.; Singhvi, G.; Dubey, S. K. Formulating Ternary Inclusion Complex of Sorafenib Tosylate Using β-Cyclodextrin and Hydrophilic Polymers: Physicochemical Characterization and In Vitro Assessment. *AAPS Pharm. Sci. Technol.* **2022**, *23*, 254.
(31) Suvarna, P.; Chaudhari, P.; Lewis, S. A. Cyclodextrin-Based Supramolecular Ternary Complexes: Emerging Role of Ternary Agents on Drug Solubility, Stability, and Bioavailability. *Crit. Rev. Ther. Drug Carrier Syst.* **2022**, *39*, 1−50.
(32) Ibrahim, M.; Munir, S.; Ahmed, S.; Chughtai, A. H.; Ahmad, W.; Khan, J.; Murtey, M. D.; Ijaz, H.; Ojha, S. C. Gliclazide in Binary and Ternary Systems Improves Physicochemical Properties, Bioactivity, and Antioxidant Activity. *Oxid. Med. Cell. Longevity* **2022**, *2022*, No. 2100092.
(33) Guo, Y.; Luo, J.; Tan, S.; Otieno, B. O.; Zhang, Z. The applications of Vitamin E TPGS in drug delivery. *Eur. J. Pharm. Sci.* **2013**, *49*, 175−186.
(34) Srivalli, K. M. R.; Mishra, B. Improved Aqueous Solubility and Antihypercholesterolemic Activity of Ezetimibe on Formulating with Hydroxypropyl-β-Cyclodextrin and Hydrophilic Auxiliary Substances. *AAPS Pharm. Sci. Technol.* **2016**, *17*, 272.
(35) Higuchi, T.; Connors, K. A. Phase Solubility Techniques. *Adv. Anal. Chem. Instrum.* **1965**, *4*, 117−212.
(36) Sherje, A. P.; Kulkarni, V.; Murahari, M.; Nayak, U. Y.; Bhat, P.; Suvarna, V.; Dravyakar, B. Inclusion Complexation of Etodolac with Hydroxypropyl-betacyclodextrin and Auxiliary Agents: Formulation Characterization and Molecular Modeling Studies. *Mol. Pharmaceutics* **2017**, *14*, 1231−1242.
(37) https://pubchem.ncbi.nlm.nih.gov/compound/silymarin.
(38) Grebogi, I.; Tibola, A. V.; Barison, A.; Grandizoli, C. P. S.; Ferraz, H.; Rodrigues, L. C. Binary and ternary inclusion complexes of dapsone in cyclodextrins and polymers: preparation, characterization and evaluation. *J. Inclusion Phenom. Macrocycl. Chem.* **2012**, *73*, 467−474.
(39) Eid, E. E. M.; Almaiman, A. A.; Alshehade, S. A.; Alsalemi, W.; Kamran, S.; Suliman, F. O.; Alshawsh, M. A. Characterization of Thymoquinone-Sulfobutylether-β-Cyclodextrin Inclusion Complex for Anticancer Applications. *Molecules* **2023**, *28*, 4096.
(40) de Freitas, M. R.; Rolim, L. A.; Soares, M. F.; Rolim-Neto, P. J.; Albuquerque, M. M.; Soares-Sobrinho, J. L.; de Albuquerque, M. M.; Soares-Sobrinho, J. L. Inclusion complex of methyl-β-cyclodextrin and olanzapine as potential drug delivery system for schizophrenia. *Carbohydr. Polym.* **2012**, *89*, 1095−1100.
(41) Shriram, R. G.; Moin, A.; Alotaibi, H. F.; Khafagy, E. S.; Saqr, A. A.; Lila, A. S. A.; Charyulu, R. N. Phytosomes as a Plausible Nano-Delivery System for Enhanced Oral Bioavailability and Improved Hepatoprotective Activity of Silymarin. *Pharmaceuticals* **2022**, *15*, 790.
(42) Hirlekar, R. S.; Sonawane, S. N.; Kadam, V. J. Studies on the effect of water-soluble polymers on drug-cyclodextrin complex solubility. *AAPS Pharm. Sci. Technol.* **2009**, *10*, 858−863.
(43) Lakshman, J. P.; Cao, Y.; Kowalski, J.; Serajuddin, A. T. Application of melt extrusion in the development of a physically and chemically stable high-energy amorphous solid dispersion of a poorly water-soluble drug. *Mol. Pharmaceutics* **2008**, *5*, 994−1002.
(44) Mennini, N.; Maestrelli, F.; Cirri, M.; Mura, P. Analysis of physicochemical properties of ternary systems ofoxaprozin with randomly methylated-ß-cyclodextrin and l-arginine aimed to improve the drug solubility. *J. Pharm. Biomed. Anal.* **2016**, *129*, 350−358.
(45) Figueiras, A.; Carvalho, R. A.; Ribeiro, L.; Torres-Labandeira, J. J.; Veiga, F. J. Solid-state characterization and dissolution profiles of the inclusion complexes of omeprazole with native and chemically modified b-cyclodextrin. *Eur. J. Pharm. Biopharm.* **2007**, *67*, 531−539.
(46) Lian, R.; Lu, Y.; Qi, J.; Tan, Y.; Niu, M.; Guan, P.; Hu, F.; Wu, W. Silymarin Glyceryl Monooleate/Poloxamer 407 liquid crystalline matrices: physical characterization and enhanced oral bioavailability. *AAPS Pharm. Sci. Technol.* **2011**, *12*, 1234−1240.
(47) Kim, S. H.; Choo, G. S.; Yoo, E. S.; Woo, J. S.; Lee, J. H.; Han, S. H.; Jung, S. H.; Kim, H. J.; Jung, J. Y. Silymarin inhibits proliferation of human breast cancer cells via regulation of the MAPK signaling pathway and induction of apoptosis. *Oncol. Lett.* **2021**, *21*, 492.

https://doi.org/10.1021/acsomega.3c04225
ACS Omega XXXX, XXX, XXX−XXX